 CMES, vol.82, no.3, pp.179-194, 2011

A New Homotopy Perturbation Method for Solving an Ill-Posed Problem of Multi-Source Dynamic Loads Reconstruction

Linjun Wang[1], **Xu Han**[2] **and Youxiang Xie**[3]

Abstract: In this paper, a new homotopy perturbation method (IHPM) is presented and suggested to solve an ill-posed problem of multi-source dynamic loads reconstruction. We propose a stable and reliable modification, and obtain a new regularization method, then employ it to find the exact solution for the multi-source dynamic load identification problem. Also, this present method only needs easy computations rather than successive integrations. Finally, the performances of two numerical examples are given. Comparisons are performed between the original homotopy perturbation method (HPM) and IHPM. The results verify that the present method is very simple and effective.

Keywords: Load identification; Ill-posed problems; Homotopy perturbation method; System of integral equations of the first kind

1 Introduction

Many engineering applications have widely concerned different kinds of load identification problems. As an important branch of inverse problems, the aim of dynamic load identification is to predict the unknown load acting on the structure by measuring the features of the system, such as the dynamic responses of structure, velocity, acceleration and strain. Many researchers have developed many different methods to identify the expected load applied to the structure in the area of structural dynamics. Cao et al. presented the method of artificial neural network to identify the loads acting on aircraft wings Cao et al (1998). Some researchers

[1] College of Mechanical and Material Engineering, China Three Gorges University, Yichang, Hubei 443002, PR China
[2] State Key Laboratory of Advanced Design and Manufacturing for Vehicle Body, College of Mechanical and Automotive Engi- neering, Hunan University, Changsha City 410082, PR China
[3] College of Mathematics and Econometrics, Hunan University, Changsha, Hunan 410082, PR China

proposed an approximate method to identify the axial forces in tie-beams by exploiting both static deflections and vibration frequencies Blasi and Sorace (1994); Sorace (1996). Lagomarsino developed a numerical method using the first three modal frequencies to identify the tensile force and the beam bending stiffness Lagomarsino and Calderini (2005). In addition, sensitivity-based methods are presented to reconstruct both plane- and space-frame forces Park et al (2006); Greening and Lieven (2003); Bahra and Greening (2006).

Moreover, in general terms, direct measurement for distributed dynamic loads is not available. However, in practical engineering problems, sometimes it is necessary and important to reconstruct the distributed dynamic loads on a continuum. Unfortunately, they are complex inverse problems with inherent ill-posedness. Regularization methods usually well control a level of numerical accuracy to obtain the true solutions of these inverse problems. From these studies mentioned above, much attention should be paid to the complicated technical problems in mathematics, especially in the ill-posedness and regularization methods. Recently, many works have been done for regularization of linear ill-posed problems Engl et al (2003); Hofmann (1986); Louis (1989); Tikhonov and Arsenin (1977). We are concerned with the problem of determining the true solution $x^\dagger$ for linear ill-posed problem

$$Ax = y, \quad (y \in R(A)) \tag{1.1}$$

where A is a bounded, non-negative, self-adjoint and injective operator on a Hilbert space X and $y \in R(A)$, the range of A. This problem is generally ill-posed in the sense that even if a unique solution for (1.1) exists, the solution may not depend continuously on the data y. This situation occurs if $R(A)$ is not closed. For each $\delta > 0$, let $y^\delta \in X$ be such that

$$\|y - y^\delta\| \le \delta \tag{1.2}$$

and known noise level δ.

In general, the problem of solving (1.1) is ill-posed. By ill-posedness, we always mean that the solution doesn't depend continuously on the data. In the case of multiple solutions, this is understandable in the sense of multivalued mappings. So it is necessary to develop some inverse analysis techniques for dealing with this kind of ill-posedness. Recently, in mathematical theory, many researchers have tried to solve these technology problems in the ill-posedness and regularization methods Choi et al (2006); Engl (1987); Gunawan et al (2006); Hilgers and Bertram (2004). An augmented Galerkin method was suggested to solve the first kind Fredholm integral equations problem which is often ill-posed Babolian and Delves (1979). Many researchers solve these ill-posed problems using wavelet basis method Walter and Shen (2001); Burrus et al (1998); Resnikoff and Wells

(1998). He first proposed the Homotopy perturbation method to solve these ill-posed inverse problems He (1999, 2000, 2003), then scientists and engineers developed and improved it Gorji et al (2007). The method combines the homotopy in topology and traditional perturbation method, and deforms continuously to a simple problem which is easily solved. Meanwhile, it significantly provides an analytical approximate solution to a wide range of linear problems in applied sciences. However, these methods are only limited to solve the pure mathematical numerical examples without application to practical engineering problems, and they should be improved to exclude jamming of noises in engineering. Moreover, for solving the ill-posed problems of dynamic load identification by them, as we know, very few papers can be found and very limited. In this paper, we intend to propose a new homotopy perturbation method for the ill-posed problems of Fredholm integral equation and apply it to the load identification problems of practical engineering.

This paper is organized as follows: In Section 2, we establish a new homotopy perturbation method, and prove the stability and convergence of the present method. Section 3 devotes to demonstrating the effectiveness of the present method using a numerical test. In Section 4, the present scheme is applied to the multi-source dynamic loads identification problem of the wing. We summarize the present method and its advantages in Section 5.

2 The establishment of a new homotopy perturbation method

In this section, we will establish a new homotopy perturbation method for solving the ill-posed problems of Fredholm integral equations of the first kind basing on the basic idea of HPM. Firstly, we consider the following system of linear equation

$$\mathbf{A}\mathbf{x} = \mathbf{b}, \tag{2.1}$$

where

$$\mathbf{A} = [a_{ij}], \quad \mathbf{x} = [x_j], \quad \mathbf{b} = [b_i], \quad i, j = 1, 2, \cdots.$$

To explain the HPM, we choose the following equation:

$$L(\mathbf{u}) = \mathbf{A}\mathbf{u} - \mathbf{b} = \mathbf{0}. \tag{2.2}$$

We may construct a convex homotopy

$$H(\mathbf{u}, p) = (1-p)F(\mathbf{u}) + pL(\mathbf{u}) = \mathbf{0} \tag{2.3}$$

It is easy to check that the solution $\mathbf{u}$ of (2.2) is also $\mathbf{x}$.

$$H(\mathbf{u}, 0) = F(\mathbf{u}), \quad H(\mathbf{u}, 1) = L(\mathbf{u}), \tag{2.4}$$

where $F(\mathbf{u})$ is a functional operator with zero point $\mathbf{u_0}$, which is not difficult to obtain. Hence, $H(\mathbf{u},p)$ continuously traces an implicitly defined curve from a starting point $H(\mathbf{u_0},0)$ to the solution function $H(\mathbf{u},1)$. The embedding parameter p monotonously increases from zero to one as the trivial problem $F(\mathbf{u})=0$ continuously deforms to original problem $L(\mathbf{u})=\mathbf{0}$. In some references He (2001); He and Wu (2006); He (2006); Chun (2007), the embedding parameter $p\in[0,1]$ can be considered as an expanding parameter to obtain

$$\mathbf{u}=\sum_{i=0}^{\infty}p^i\mathbf{u_i}=\mathbf{u_0}+p\mathbf{u_1}+p^2\mathbf{u_2}+\cdots. \tag{2.5}$$

When $p\to1$, (2.3) corresponds to (2.2) and becomes the approximate solution of (2.2), i.e.,

$$\mathbf{x}=\lim_{p\to1}\mathbf{u}=\sum_{i=0}^{\infty}\mathbf{u_i}. \tag{2.6}$$

Let $F(\mathbf{u})=\alpha\mathbf{u}-\mathbf{w_0}$, by substituting (2.5) into (2.3) and equating the terms with identical powers of p, we have

$$\begin{array}{lll} p^0 & : & \alpha\mathbf{u_0}-\mathbf{w_0}=\mathbf{0},\quad \alpha\mathbf{u_0}=\mathbf{w_0},\\ p^1 & : & (\mathbf{A}-\alpha\mathbf{I})\mathbf{u_0}+\alpha\mathbf{u_1}+\mathbf{w_0}-\mathbf{b}=\mathbf{0},\quad \mathbf{u_1}=\frac{\alpha-\mathbf{A}}{\alpha}\mathbf{u_0}+\frac{\mathbf{b}-\mathbf{w_0}}{\alpha},\\ p^2 & : & (\mathbf{A}-\alpha\mathbf{I})\mathbf{u_1}+\alpha\mathbf{u_2}=\mathbf{0},\quad \mathbf{u_2}=\frac{\alpha-\mathbf{A}}{\alpha}\mathbf{u_1},\\ p^3 & : & (\mathbf{A}-\alpha\mathbf{I})\mathbf{u_2}+\alpha\mathbf{u_3}=\mathbf{0},\quad \mathbf{u_3}=\frac{\alpha-\mathbf{A}}{\alpha}\mathbf{u_2}, \end{array} \tag{2.7}$$

and in general

$$\mathbf{u_{n+1}}=\frac{\alpha-\mathbf{A}}{\alpha}\mathbf{u_n},\quad n=1,2,\cdots. \tag{2.8}$$

If we take $\mathbf{u_0}=\mathbf{w_0}=\mathbf{0}$, then we have

$$\begin{array}{rcl} \mathbf{u_1} & = & \frac{\mathbf{b}}{\alpha},\\ \mathbf{u_2} & = & \frac{\alpha-\mathbf{A}}{\alpha}\cdot\frac{1}{\alpha}\cdot\mathbf{b},\\ \mathbf{u_3} & = & (\frac{\alpha-\mathbf{A}}{\alpha})^2\cdot\frac{1}{\alpha}\cdot\mathbf{b},\\ \vdots & & \\ \mathbf{u_{n+1}} & = & (\frac{\alpha-\mathbf{A}}{\alpha})^n\cdot\frac{1}{\alpha}\cdot\mathbf{b}. \end{array} \tag{2.9}$$

Therefore, the true solution can be given as

$$\mathbf{u}=\sum_{i=0}^{\infty}(\frac{\alpha\mathbf{I}-\mathbf{A}}{\alpha})^i\cdot\frac{1}{\alpha}\cdot\mathbf{b}=\left[\mathbf{I}+(\frac{\alpha\mathbf{I}-\mathbf{A}}{\alpha})+(\frac{\alpha\mathbf{I}-\mathbf{A}}{\alpha})^2+\cdots\right]\cdot\frac{1}{\alpha}\cdot\mathbf{b}. \tag{2.10}$$

Theorem 2.1. The sequence $\mathbf{u}^{[\mathbf{n}]} = \sum_{i=0}^{\infty} (\frac{\alpha\mathbf{I}-\mathbf{A}}{\alpha})^i \cdot \frac{1}{\alpha} \cdot \mathbf{b}$ is a Chauchy sequence if $\|\frac{\mathbf{A}}{\alpha} - \mathbf{I}\| < 1$.

Proof. It is easy to check that

$$\mathbf{u}^{[\mathbf{n+p}]} - \mathbf{u}^{[\mathbf{n}]} = \sum_{i=1}^{p} (\frac{\alpha\mathbf{I}-\mathbf{A}}{\alpha})^{n+i} \cdot \frac{1}{\alpha} \cdot \mathbf{b}.$$

Then

$$\|\mathbf{u}^{[\mathbf{n+p}]} - \mathbf{u}^{[\mathbf{n}]}\| \leq \|\mathbf{b}\| \sum_{i=1}^{p} \|\frac{\mathbf{A}-\alpha\mathbf{I}}{\alpha}\|^{n+i} \cdot \frac{1}{|\alpha|}.$$

Set $\|\frac{\mathbf{A}}{\alpha} - I\| = \eta$. Thus we can obtain

$$\|\mathbf{u}^{[\mathbf{n+p}]} - \mathbf{u}^{[\mathbf{n}]}\| \leq \frac{1}{|\alpha|} \|\mathbf{b}\| \eta^n \sum_{i=1}^{p} \eta^i \leq \frac{\|\mathbf{b}\|}{|\alpha|} \eta^n \frac{1-\eta^p}{1-\eta}.$$

So

$$\lim_{n\to\infty} \|\mathbf{u}^{[\mathbf{n+p}]} - \mathbf{u}^{[\mathbf{n}]}\| \leq \lim_{n\to\infty} \frac{\|\mathbf{b}\|}{|\alpha|} \frac{1-\eta^p}{1-\eta} \eta^n = \frac{\|\mathbf{b}\|}{|\alpha|} \frac{1-\eta^p}{1-\eta} \lim_{n\to\infty} \eta^n = 0.$$

Now the result of Theorem 2.1 can be proved easily.

Remark 2.1. In practice, all terms of series (2.6) cannot be determined and so we define an approximation of the solution by the following truncated series:

$$\mathbf{u} = \sum_{i=0}^{m-1} (\frac{\alpha\mathbf{I}-\mathbf{A}}{\alpha})^i \cdot \frac{1}{\alpha} \cdot \mathbf{b}. \tag{2.11}$$

Similar to the analysis that regularization is the approximation of an ill-posed problem by a family of neighboring well-posed problems, it constructs a new positive matrix approximating the original singular matrix, then the stable and efficient regularized solution is obtained. Thus IHPM is established and does not depend on the iterations. Moreover, it is also a stable and effective regularization method. The term n plays the role of regularization parameter.

3 Benchmark test

In this section, we will validate herein the present method detailed in previous section with the following numerical example. We consider the first kind of Fredholm integral equation

$$\int_0^1 e^{ts} x(s) ds = \frac{e^{t+1}-1}{t+1}, \quad t \in [0,1]. \tag{3.1}$$

It is easy to check that the true solution of Eq.(3.1) is $x(s) = e^s$. In general terms, we need to solve the perturbed equation

$$\int_0^1 e^{ts}x(s)ds = y^\delta(t), \quad t \in [0,1]. \tag{3.2}$$

Discretizing Eq. (3.2), we can obtain

$$\frac{1}{N}\sum_{j=1}^{N} e^{t_i s_j}x(s_j) = y_i^\delta, \quad i,j = 1,2,\cdots,N, \tag{3.3}$$

where

$$t_i = \frac{i-1}{N}, s_j = \frac{j-1}{N}, y_i^\delta = y(t_i) + \theta_i\delta,$$

θ_i is a random number and satisfies $|\theta_i| \leq 1$.

To analyze the convergence performances of the present method, we denote $N = 50$ as the number of grid and choose noisy level $\delta = 0.05$. Applying PC-MATLAB environment, we obtain the following results.

The comparison of the true solution with the numerical results by HPM method and IHPM is illustrated in Figure 1 and Table 1. From these numerical simulations, we conclude that the present method works better than HPM. We managed to solve the ill-posed problem by IHPM with acceptable accuracy. This shows that the proposed algorithm is easy, effective and stable.

Table 1: The errors of numerical solutions at the noise level $\delta = 0.05$

	Noise level 0.05	
	Maximum Error (%)	Average Error (%)
HPM method	0.6292	0.3813
Present method	0.1958	0.1191

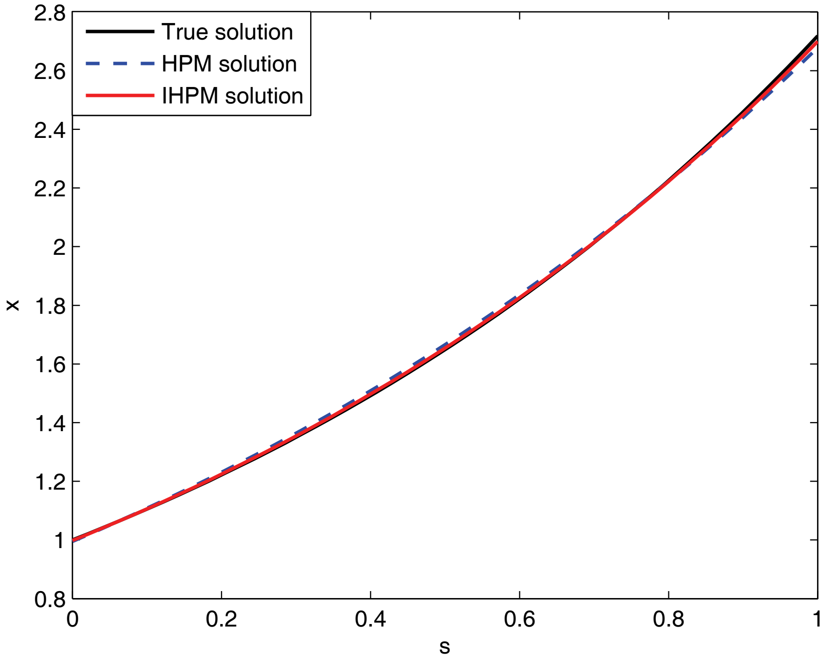

Figure 1: Numerical solutions at the noise level $\delta = 0.05$

4 Application

To illustrate the present methodology for use in determining the unknown time-dependent multi-source dynamic loads acting on the wing, we need to know the following knowledge for a linear elastic structure.

Here we consider the multi-source dynamic load identification problem for a linear and time-invariant dynamic system. The response at an arbitrary receiving point in a structure can be expressed as a convolution integral of the forcing time-history and the corresponding Green's kernel in time domain Liu and Han (2003); Liu et al (2002):

$$y(t) = \int_0^t G(t-\tau)p(\tau)d\tau, \tag{4.1}$$

where $y(t)$ is the response which can be displacement, velocity, acceleration, strain, etc. $G(t)$ is the corresponding Green's function, which is the kernel of impulse response. $p(t)$ is the desired unknown dynamic load acting on the structure.

By discretizing this convolution integral, the whole concerned time period is separated into equally spaced intervals, and the equation (4.1) is transformed into the following system of algebraic equation:

$$Y(t) = G(t)P(t), \tag{4.2}$$

or equivalently,

$$\begin{pmatrix} y_1 \\ y_2 \\ \vdots \\ y_m \end{pmatrix} = \begin{pmatrix} g_1 & & & \\ g_2 & g_1 & & \\ \vdots & \vdots & \ddots & \\ g_m & g_{m-1} & \cdots & g_1 \end{pmatrix} \begin{pmatrix} p_1 \\ p_2 \\ \vdots \\ p_m \end{pmatrix} \triangle t,$$

where y_i, g_i, and p_i are response, Green's function matrix and input force at time $t = i\triangle t$, respectively. $\triangle t$ is the discrete time interval. Since the structure without applied force is static before force is applied, y_0 and g_0 are equal to zero. All the elements in the upper triangular part of G are zeros and are not shown. The special form of the Green's function matrix reflects the characteristic of the convolution integral.

To recover the time history $P(t)$, the knowledge of $y(t)$ and $G(t)$ are required. In fact, the response at a receiving point and the numerical Green's function of a structure can be obtained by finite element method. However, the problem of identifying the dynamic load $P(t)$ by $y(t)$ and $G(t)$ is usually ill-posed, and cannot be solved by inverse matrix method. In the following, our method will be suggested to solve this problem.

A practical engineering problem is to determine vertical forces acting on the out surface of the wing, which is shown in Figure 2. The material properties of the wing are as: $E = 3.8 \times 10^{11} Mpa$, $\nu = 0.3$, $\rho = 8.3 \times 10^3 kg/m^3$.

The vertical concentrated load is applied to the outside surface and the measured response is the vertical displacement. One side of it is free, and the other side is fixed. We establish its finite element model as shown in Figure 2. The arrow in Figure 2 denotes the point of dynamic force.

The concentrated loads are defined as follows:

$$\begin{aligned} F_1(t) &= \begin{cases} q_1 \sin(\frac{2\pi t}{t_d}), & 0 \le t \le 2t_d \\ 0, & t < 0 \quad and \quad t > 2t_d \end{cases} \\ F_2(t) &= \begin{cases} 4q_2 t/t_d, & 0 \le t \le t_d/4 \\ 2q_2 - 4q_2 t/t_d, & t_d/4 < t \le 3t_d/4 \\ 4q_2 t/t_d - 4q_2, & 3t_d/4 < t \le t_d \\ 0, & t > t_d \end{cases} \end{aligned}$$

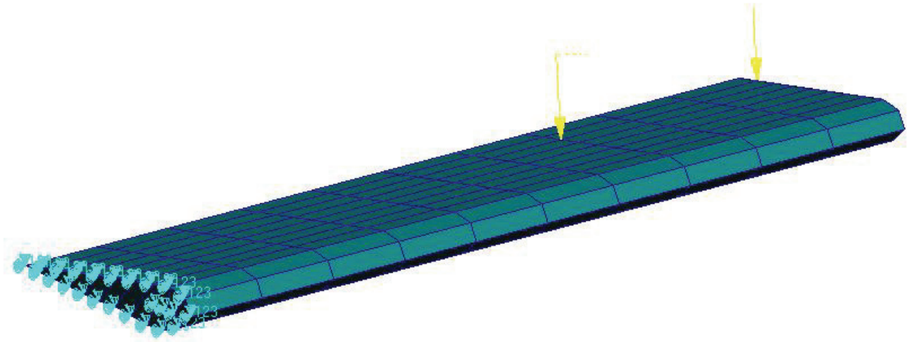

Figure 2: The finite element model of the wing

where t_d is the time cycle of sine force, and $q_i(i = 1,2)$ is a constant amplitude of the force. When $t_d = 0.004s, q_1 = 1000N$, and $q_2 = 800N$, the sine force and triangle force are shown in Figures 3-4.

Herein, the experimental data of response is simulated by the computed numerical solution, and the corresponding radial displacement response can be obtained by finite element method, as shown in Figures 5-6. Furthermore, a noise is directly added to the computer-generated response to simulate the noise-contaminated measurement, and the noisy response is defined as follows:

$$Y_{err} = Y_{cal} + l_{noise} \cdot std(Y_{cal}) \cdot rand(-1,1),$$

where Y_{cal} is the computer-generated response; $std(Y_{cal})$ is the standard deviation of Y_{cal}; $rand(-1,1)$ denotes the random number between -1 and +1; l_{noise} is a parameter which controls the level of the noise contamination. In order to investigate the effect of measurement error on the accuracy of estimated values, we consider the case of noise level namely 5% and $\alpha = 2$, then this new regularization method is suggested to determine the multi-source dynamic forces. To evaluate the effectiveness of the present method, five time points are selected, and the identified force for each point will be compared to the corresponding actual force.

The results of numerical simulations are as follows:

Numerical performances of the present method are compared with those of HPM, as are shown in Figures 7-8. From these two pictures, we can see that the present method can produce more accurate results than HPM. The other results of the identified loads at five time points are listed in Table 2. From these results given in Table 2, it can be seen that the proposed method provides accurate results and has a good

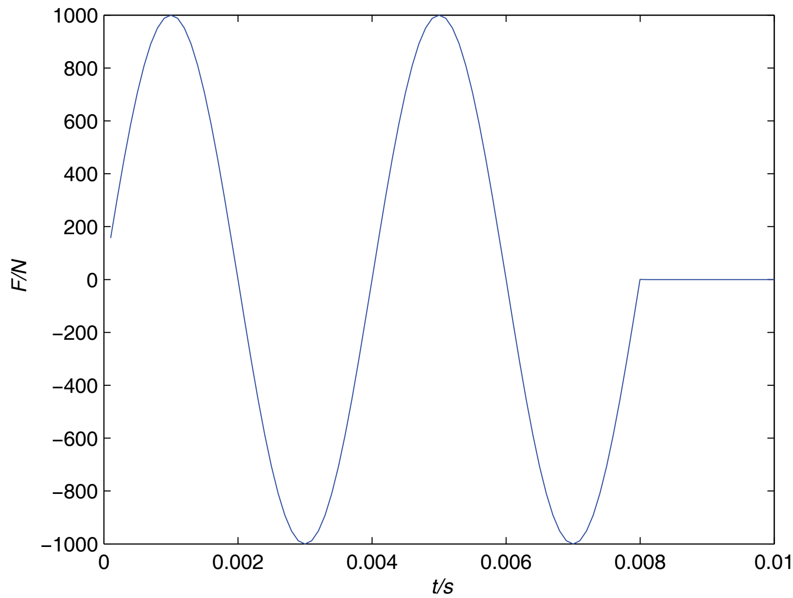

Figure 3: The radial concentrated sine load acting on the outside surface

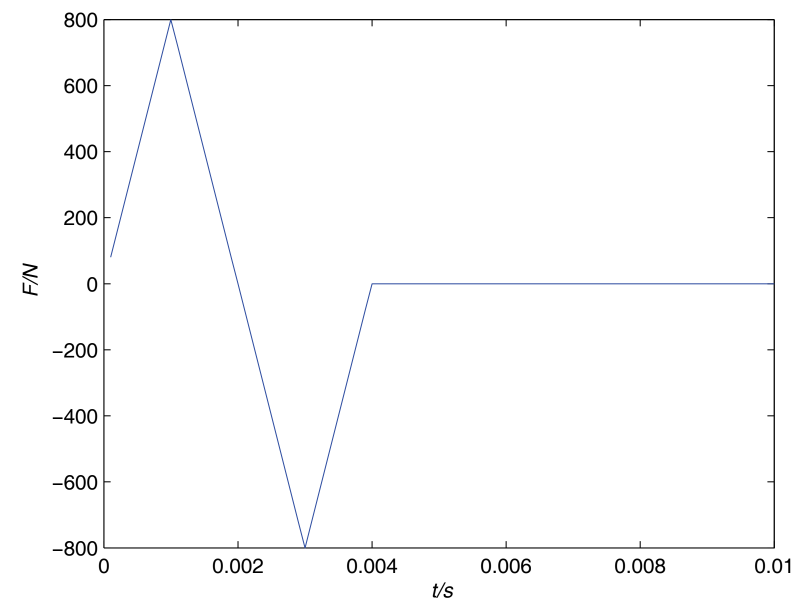

Figure 4: The radial concentrated triangle load acting on the outside surface

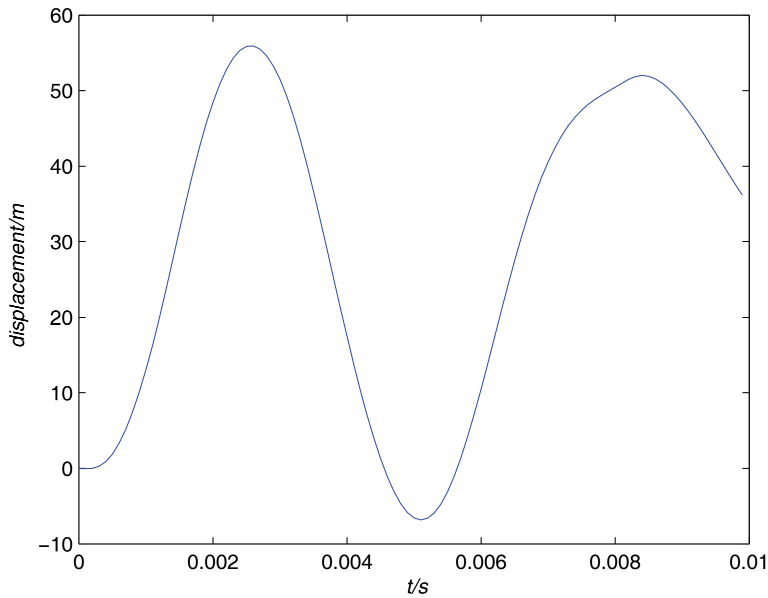

Figure 5: The corresponding vertical displacement response at one point

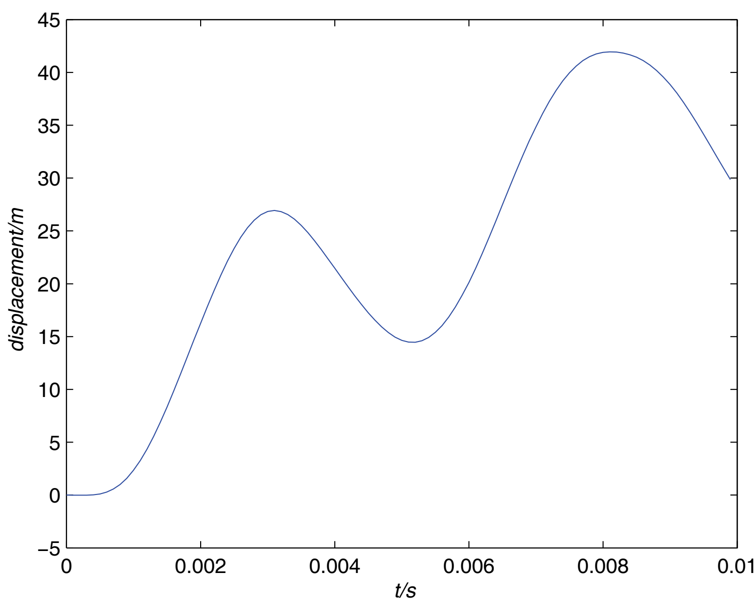

Figure 6: The corresponding vertical displacement response at the other point

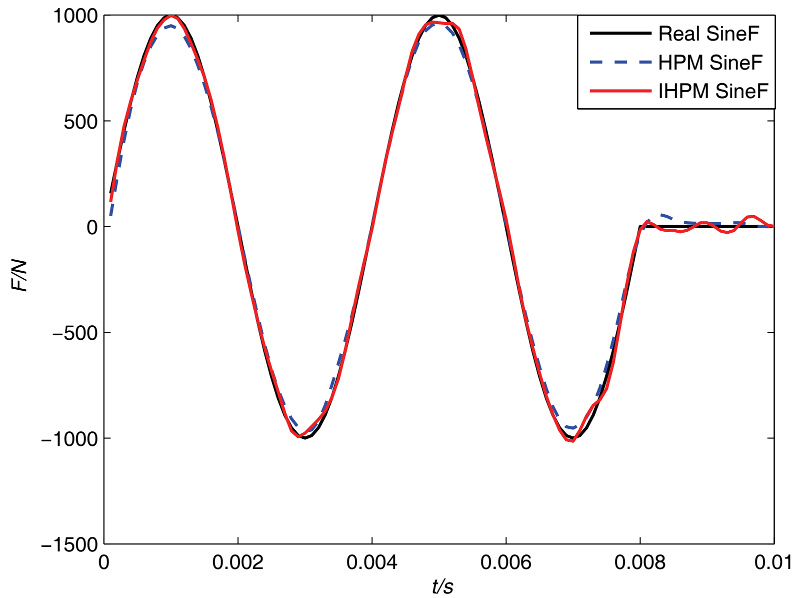

Figure 7: The identified sine force at noise level 5%

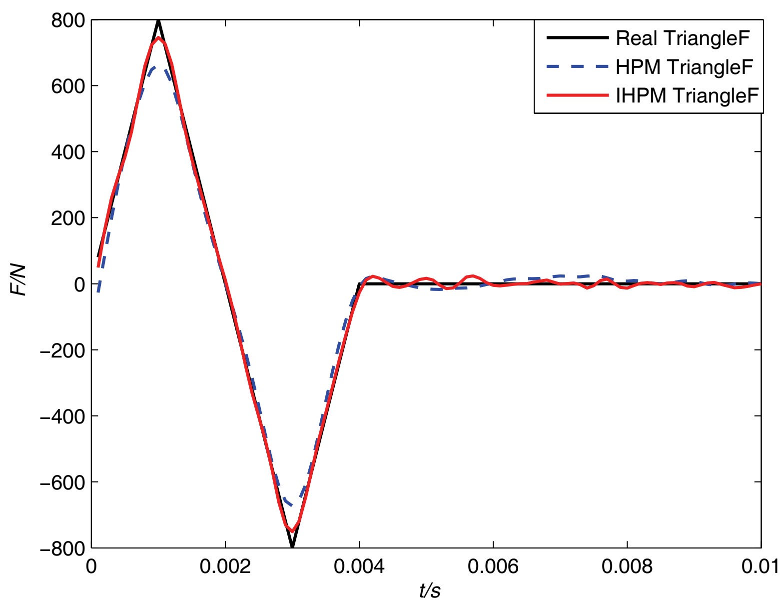

Figure 8: The identified triangle force at noise level 5%

Table 2: The identified force at five time points at noise level 5%

	Time point	Real force	HPM Identified force	HPM Error (%)	Present method Identified force	Present method Error (%)
Sine	0.001	1000	950.17	4.98	999.17	0.08
Triangle	0.0006	480	474.88	0.64	459.81	2.52
Sine	0.003	-1000	-968.65	3.14	-976.01	2.40
Triangle	0.001	800	663.82	17.02	745.59	6.80
Sine	0.0045	707.11	692.73	1.44	705.12	0.20
Triangle	0.0016	320	289.62	3.80	302.79	2.15
Sine	0.0063	-453.99	-427.53	2.65	-448.59	0.54
Triangle	0.0033	-560	-536.61	2.92	-556.68	0.42
Sine	0.0073	-891.01	-844.85	4.62	-844.88	4.61
Triangle	0.0038	-160	-111.07	6.12	-155.69	0.54
Error (%)			Maximum	Average	Maximum	Average
Sine			10.57	3.01	5.94	1.81
Triangle			17.02	2.76	6.80	1.18

convergence performance. It can be found that at these time points for noise level $\pm 5\%$, these deviations of identified loads by the present method are smaller than HPM because of efficient identification. At the time point 0.001, the true sine force is $1000N$, while the identified forces by HPM and IHPM are $950.17N, 999.17N$, respectively. Moreover, at the other time points, most of the performances of IHPM are better than HPM. Similar to the analysis above, we can obtain that IHPM performs better than HPM at most time points. It can be also found that most of the errors by HPM and the present method concentrate in the range of $17.02\%, 6.80\%$, respectively. Also, for the identification of sine force, the maximal error and average error by the present method are $5.94\%, 1.81\%$, respectively, obviously smaller than HPM. In addition, the maximal error and average error of the identification of triangle force by the present method are $6.80\%, 1.18\%$, respectively, both smaller than HPM. In a word, the present algorithm is stable and effective in reconstructing the loading time function, and gives very stable and satisfactory results.

5 Conclusion

In this work, a new homotopy perturbation method is presented and considered as an alternative to approximate the true solution of the ill-posed problem of multi-source dynamic loads reconstruction. In this new modification, a new homotopy $H(\mathbf{u}, p, \alpha)$ was constructed, where α is called the accelerating parameter. A fast convergent rate will be obtained due to the accelerating parameter, and then the numerical solutions approach the exact solution. Meanwhile, numerical simulations of two examples show that the present method is a very fast convergent, precise and cost efficient tool for solving the ill-posed problems of load identification in practical engineering.

Acknowledgement: This work is supported by the National Science Foundation of China for Distinguished Young Scholars (10725208), the Foundation of China Three Gorges University (KJ2011B033) and Research Fund for National 973 Project of China (2010CB832705). The authors thank the anonymous referees and the editor for carefully reading this paper and suggesting many helpful comments on improving the original manuscript.

References

Babolian E, Delves LM. (1979): An augmented Galerkin method for first kind Fredholm equations. *J. Inst. Math. Appl.* 12: 157-174.

Bahra, A.S., Greening, P.D. (2006): Particularities of Newton¡¯s method in space frame force determination utilising eigenpair functions, *Journal of Sound and Vibration* 291 (1-2), 462-490.

Blasi, C., Sorace, S. (1994): Determining the axial force in metallic rods, *Structural Engineering International* 4 (4), 241-246.

Burrus CS, Gopinath RA, Guo H. (1998): *Introduction to Wavelets and Wavelet Transforms*. Prentice Hall.

Cao, X., Sugiyama Y., Mitsui, Y. (1998): Application of artificial neural networks to load identification, *Computers and Structures*, 69, 63-78.

Choi HG, Thite AN, Thompson DJ. (2006): A threshold for the use of Tikhonov regularization in inverse force determination. *Applied Acoustics* 67 (7): 700-719.

Chun CB. (2007): Integration using He's homotopy perturbation method. Chaos, *Solitons and Fractals* 34: 1130-1134.

Engl HW. (1987): Discrepancy Principles for Tikhonov Regularization of Ill-Posed Problems Leading to Optimal Convergence Rates. *Journal of Optimization Theory and Applications* 52: 209-215.

Engl HW, Hanke M, Neubauer A. (2003): *Regularization of Inverse Problems*. Dordrecht: Kluwer.

Gorji M, Ganji DD, Soleimani S. (2007): New application of He's homotopy perturbation method. *Int. J. Nonlinear Sci. Numer. Simul.* 8: 319-328.

Greening, P.D., Lieven, N.A.J. (2003): Identification and updating of loading in frameworks using dynamic measurements, *Journal of Sound and Vibration* 260 (1), 101-115.

Gunawan FE, Homma H, Kanto Y. (2006): Two-step B-splines regularization method for solving an ill-posed problem of impact-force reconstruction. *Journal of Sound and Vibration* 297 (1-2): 200-214.

He JH. (1999): Homotopy perturbation technique. *Comput. Methods. Appl. Mech. Eng.*; 178: 257-262.

He JH. (2000): A coupling method of homotopy technique and perturbation technique for nonlinear problems. *Int. J. Non-Linear Mech* 35: 37-43.

He JH. (2001): Iteration perturbation method for strongly nonlinear oscillations. *J. Vib. Control* 7: 631-642.

He JH. (2003): Homtopy perturbation method: a new nonlinear analytic technique. *Appl. Math. Comput.* 135: 73-79.

He JH. (2006): Some asymptotic methods for strongly nonlinear equations. *In. J. Mod. Phys. B* 20: 1141-1199.

He JH, Wu XH. (2006): Exp-function method for nonlinear wave equations. Chaos, *Solitons and Fractals* 30: 700-708.

Hilgers JW, Bertram BS. (2004): Comparing different types of approximations for choosing the parameters in the regularization of ill-posed problems. *Computers and Mathematics with Applications* 48: 1779-1790.

Hofmann B. (1986): *Regularization of Applied Inverse and Ill-Posed Problems*. Leipzig: Teubner.

Lagomarsino, S., Calderini, C. (2005): The dynamical identification of the tensile force in ancient tie-rods, *Engineering Structures* 27 (6), 846-856.

Liu, G. R., Han, X. (2003): *Computational inverse technique in nondestructive evaluation*, CRC Press, Florida.

Liu, G. R., Ma, W. B., Han, X. (2002): An inverse procedure for identification of loads on composite laminates, *Composites Part B: engineering* 33: 425-432.

Louis AK. (1989): *Inverse und schlecht gestellte Probleme*. Stuttgart: Teubner.

Park, S., Choi, S., Oh, S.T., Stubbs, N., Song, H.C. (2006): Identification of the tensile force in high-tension bars using modal sensitivities, *International Journal of Solids and Structures* 43 (10), 3185-3196.

Resnikoff HL, Wells RO. (1998): *Wavelet Analysis*. New York: Springer.

Sorace, S. (1996): Parameter models for estimating in-situ tensile force in tie-rods, *Journal of Engineering Mechanics* 122 (9), 818-825.

Tikhonov AN, Arsenin VY. (1977): *Solution of Ill-Posed Problems*. New York: Wiley.

Walter GG, Shen X. (2001): *Wavelets and Other Orthogonal Systems*, second ed., Chapman and Hall/CRC.